Experimental and theoretical results of room-temperature single-electron transistor formed by the atomic force microscope nano-oxidation process*

Y. Gotoh,[a] K. Matsumoto, and T. Maeda
Electrotechnical Laboratory MITI, 1-1-4 Umezono, Tsukuba, Ibaraki 305-8568, Japan

E. B. Cooper and S. R. Manalis
Massachusetts Institute of Technology, Cambridge, Massachusetts 02139

H. Fang
Columbia University, 3000 Broadway, New York, New York 10027

S. C. Minne, T. Hunt, H. Dai, J. Harris, and C. F. Quate
Stanford University, Stanford, California 94305

(Received 4 October 1999; accepted 24 April 2000)

The single-walled carbon-nanotube (SWNT) was grown directly onto the top of the conventional Si atomic force microscopy (AFM) cantilever. This SWNT AFM cantilever was introduced into the AFM nano-oxidation process, which oxidized the titanium (Ti) metal film on the atomically flat α-Al_2O_3 substrate and formed the ultranarrow oxidized titanium (TiO_x) line of 5 nm width. This TiO_x line was used as the tunnel junction of the single-electron transistor (SET), and the SET fabricated by this process showed room-temperature Coulomb oscillation with periods of 1 V. It was determined by three-dimensional simulation that the tunnel-junction capacitance shows only weak dependence on the tunnel-junction width. © *2000 American Vacuum Society.*
[S0734-2101(00)17004-6]

I. INTRODUCTION

Various types of single-electron transistors (SETs)[1–6] were proposed for room-temperature operation. The SETs were based on the Coulomb blockade phenomena, and the electron can be controlled one by one. Some devices use the nanometer-sized structure fabricated by using a spontaneously formed structure, such as a polysilicon thin layer[1] or an ultrathin Si layer. Other devices use an artificial nanostructure via the application of e-beam lithography, followed by angle metal evaporation.[3] We have thus far fabricated the nanostructure of room-temperature SETs[4–6] by an atomic force microscope (AFM) nano-oxidation process.[7–9] In our present article, for the better characteristics of the SET at room temperature, we calculated the dependence of the tunnel-junction capacitance on the structure of the SET. We found an important relation between the tunnel-junction width and the tunnel-junction capacitance using three-dimensional simulation. To realize this important result of three-dimensional simulation, the single-walled carbon nanotube (SWNT) AFM cantilever[10,11] was introduced into our process to reduce the tunnel-junction width, and the SET was fabricated.

II. STRUCTURE OF PLANAR-TYPE, SINGLE-ELECTRON TRANSISTOR AND AFM NANO-OXIDATION PROCESS

Figures 1(a) and 1(b) show the AFM image and the schematic structure of the fabricated planar-type SET[4–6] using the AFM nano-oxidation process,[7–9] which oxidized the surface of the Ti metal film on the atomically flat α-Al_2O_3 substrate. The pulse bias was applied between the AFM cantilever and the surface of the Ti metal film, as shown in Fig. 2, and the TiO_x lines several tens of nm wide were formed just under the scanning AFM cantilever using the moisture from the ambient air as a chemical reactor. These narrow TiO_x lines were used for the tunnel junctions of the SET.

The structure of the fabricated SET has one island sandwiched by two tunnel junctions. The source drain and the gate barrier were as wide as over 1 μm to completely suppress the leakage current between the electrodes. The size of each island, the tunnel-junction width, and other parameters will be shown in Sec. V.

III. THREE-DIMENSIONAL SIMULATION

For the practical use of a room-temperature SET, a larger tunnel current (i.e., larger signal current) and a smaller tunnel capacitance are preferable. We are concerned, however, that reducing the tunnel-junction width to increase the tunnel current may increase the tunnel-junction capacitance. Therefore, the dependence of the tunnel-junction capacitance on the tunnel-junction width was estimated by three-dimensional simulation.

The structure for the simulation is the same as that of the experimental one shown in Fig. 1(b). The SET island length L (i.e., the distance between the source/drain barrier and the gate barrier) was fixed at 5 nm. The SET island width W was also fixed at 5 nm. The tunnel-junction width t was used as a variable and ranged from 30 to 5 nm. The α-Al_2O_3 substrate thickness was 2 μm and the permittivity was 7. The Ti thick-

*No proof corrections received from author prior to publication.
[a]Author to whom correspondence should be addressed; electronic mail: ygotou@xa2.so-net.ne.jp

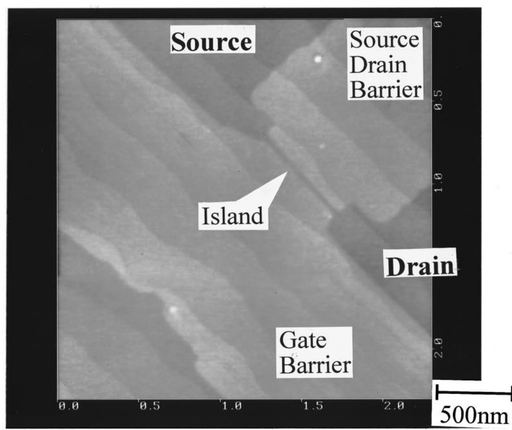

(a)

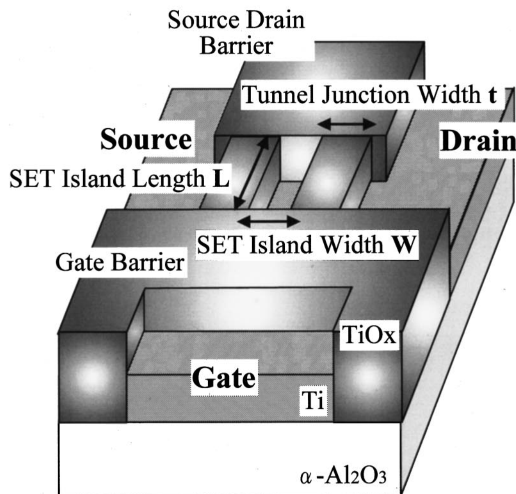

(b)

FIG. 1. (a) AFM image of one island side-gate SET fabricated by AFM nano-oxidation process on atomically flat α-Al_2O_3 substrate. (b) Schematic structure of one island side-gate SET. In fabricated SET, tunnel-junction width t and length L are 8 and 17 nm, respectively. SET island width W is 7 nm.

ness was 1 nm. The TiO_x thickness was 1 nm and the permittivity was 5. The tunnel-junction capacitance was calculated by solving the three-dimensional Poisson equation. The numerical calculation was stopped when the error ratio of the simulated results became less than 0.01%. Figure 3 shows the dependence of the tunnel-junction capacitance on the tunnel-junction width t. In this figure, the tunnel-junction capacitance shows a very weak dependence on the tunnel-junction width t, even if the tunnel-junction width is reduced from 30 to 5 nm. This result was quite different from that of the capacitance calculated using the conventional parallel-plate approximation. The reason for this discrepancy is explained as follows: in the present structure of the SET, the electric field not only penetrates through the TiO_x tunnel barrier, but also mainly through the α-Al_2O_3 substrate under the tunnel junctions because of the larger relative permittivity: the electric field in the α-Al_2O_3 substrate has a larger influence on the tunnel-junction capacitance than that in the tunnel junctions. Therefore, even when the tunnel-junction

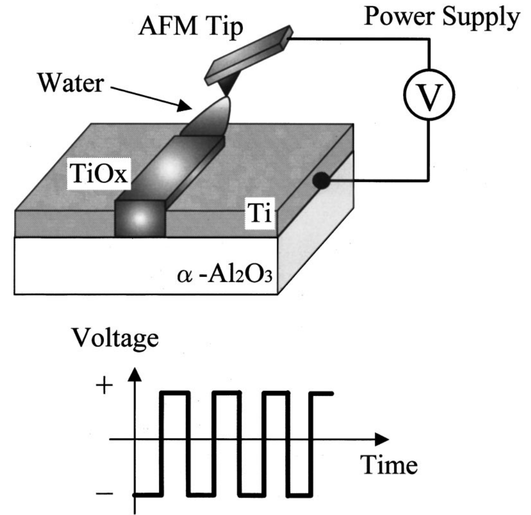

FIG. 2. Principle of AFM nano-oxidation process. Ti metal film is 2 nm in thickness, and substrate is atomically flat α-Al_2O_3. Pulse bias was applied between AFM cantilever and surface of Ti metal film, and surface of Ti is anodized to form oxidized Ti, i.e., TiO_x.

width was drastically reduced, the tunnel-junction capacitance only showed a slight change.

Consequently, we found that for the SET, the tunnel current could be increased by reducing the tunnel-junction width, without increasing the tunnel-junction capacitance.

IV. SWNT AFM CANTILEVER

To fabricate the narrower tunnel junctions, i.e., the narrower TiO_x lines, using the AFM nano-oxidation process, it is indispensable to use the sharp apex for the AFM cantilever. For this purpose, the SWNT AFM cantilever[10–14] was introduced into this process. The SWNT was grown directly onto the top of the conventional Si AFM cantilever using

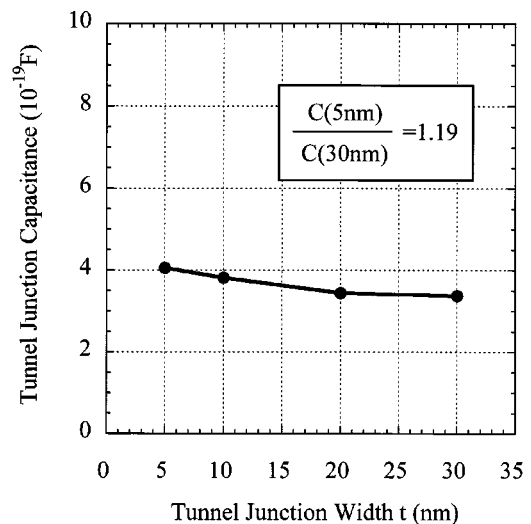

FIG. 3. Dependence of tunnel-junction capacitance on tunnel-junction width t. Tunnel-junction length L and island width W were fixed at 5 nm. Tunnel-junction capacitance shows a very weak dependence on tunnel-junction width t, even if tunnel-junction width t is reduced from 30 to 5 nm.

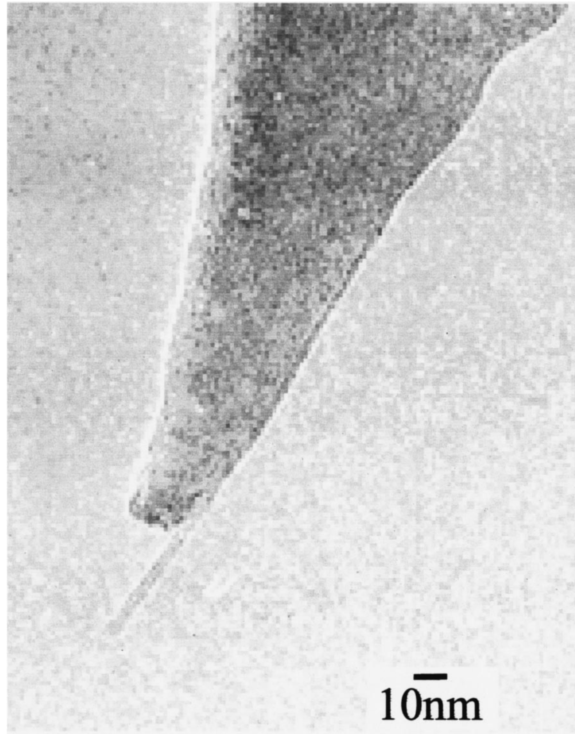

FIG. 4. TEM image of SWNT AFM cantilever, which is grown onto conventional Si AFM cantilever using CVD. Diameter of SWNT is as small as 3 nm and length is 30 nm.

chemical vapor deposition (CVD). Figure 4 shows the transmission electron microscopy (TEM) image of the top of the SWNT AFM cantilever. The size of the conventional Si AFM cantilever apex is about 20 nm. However, the diameter of the SWNT is as small as 3 nm and the length is about 30 nm.

Using the SWNT AFM cantilever, the narrow TiO_x line was formed, as shown in Fig. 5(a). The linewidth was as small as 6 nm, as shown in the cross section of Fig. 5(b), and the height was 1 nm. The fabrication conditions were as follows: the applied pulse bias between the AFM cantilever and the Ti metal film for the oxidation was -8.5 V to $+0.5$ V, the frequency was 10 Hz, and the scanning speed was 40–100 μm/s. In contrast, the TiO_x line formed by the conventional Si AFM cantilever is as wide as 19 nm, as shown in Figs. 6(a) and 6(b), because of the larger apex of the Si AFM cantilever. Consequently, using the SWNT AFM cantilever, tunnel junctions three times narrower could be formed than by using the conventional Si AFM cantilever.

The durability of the SWNT AFM cantilever was examined by fabricating the 250 TiO_x lines, as shown in Fig. 7. Each line is 5 nm in width and 5 μm in length. All TiO_x lines are continuous, and there are no cut or damarged areas. This means that the SWNT AFM cantilever shows no degradation, even after long oxidation.

V. CHARACTERISTIC OF SET FABRICATED BY SWNT AFM CANTILEVER

The SET shown in Fig. 1 was fabricated by the AFM nano-oxidation process. In particular, the two tunnel junctions were fabricated using a SWNT AFM cantilever. The island length L of the SET was 17 nm, and the island width W was 7 nm. The tunnel-junction width t was as small as 8 nm.

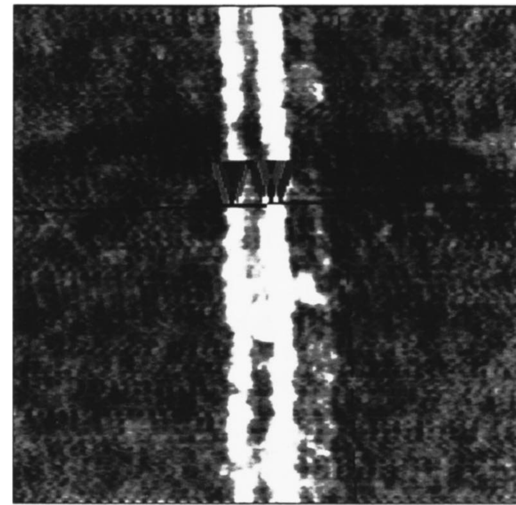

(a)

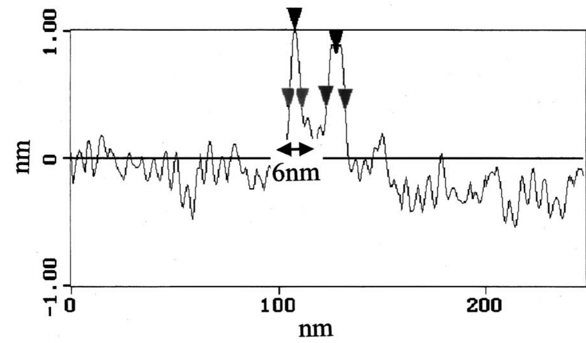

(b)

FIG. 5. (a) AFM image of two TiO_x lines fabricated by SWNT AFM cantilever at Ti film on atomically flat α-Al_2O_3 substrate. (b) Cross-sectional view of two TiO_x lines fabricated by carbon nanotube AFM cantilever. Two TiO_x linewidths are only 6 nm, and heights are 1 nm.

The Coulomb oscillation characteristic of this SET, measured at room temperature, is shown in Fig. 8. The measurement conditions were as follows: the drain bias was set at $V_D = 5.0$ V, and the gate bias was changed from $V_G = 1.0$ V–8.0 V. The periods of Coulomb oscillation are about 1 V. From the periods of this Coulomb oscillation, the gate capacitance was estimated to be 1.6×10^{-19} F. The drain current of the SET is on the order of 10^{-13} A, and the signal-to-noise ratio of the Coulomb oscillation is 3–4.

The magnitude of the drain current of the SET so far fabricated with the tunnel-junction width of about 20 nm is 10^{-15}–10^{-14} A. Therefore, in the present experiment, the slight increase of the drain current using the narrower tunnel junction made by the SWNT AFM cantilever was attained. However, the increase of the drain current is smaller than expected. The reason for this smaller increase of the drain current is not clear. One possible reason, however, is the

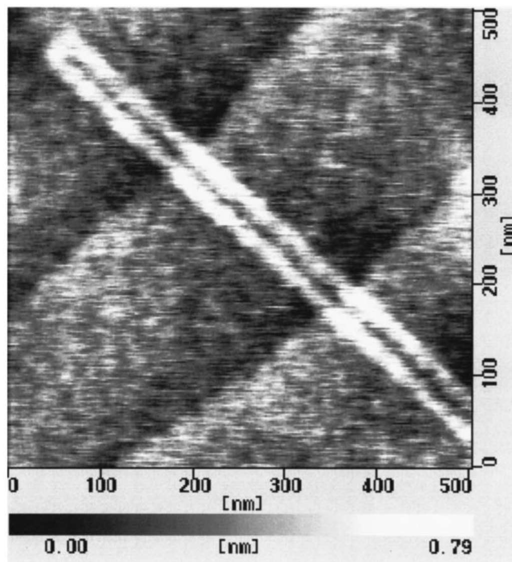

(a)

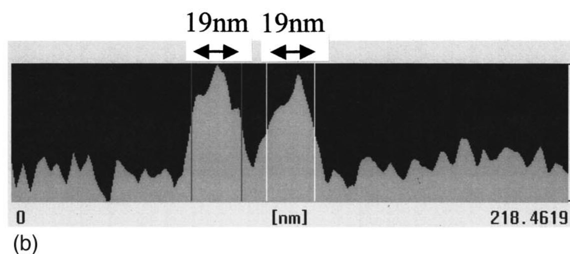

(b)

FIG. 6. (a) AFM image of two TiO_x lines fabricated by the conventional Si AFM cantilever at Ti film on atomically flat α-Al_2O_3 substrate. (b) Cross-sectional view of two TiO_x lines fabricated by conventional Si AFM cantilever. Two TiO_x linewidths are as large as 19 nm, and heights are 1 nm.

increase of the barrier height between the TiO_x and the Ti because of the different fabrication condition: i.e., the present fabrication process uses the SWNT AFM cantilever, rather than the conventional Si AFM cantilever, and the scanning speed of the SWNT AFM cantilever is 10 000 times faster than that used in the Si AFM cantilever. These different fabrication conditions may cause an increase of the TiO_x/Ti barrier height and causes a smaller increase of the drain current than expected.

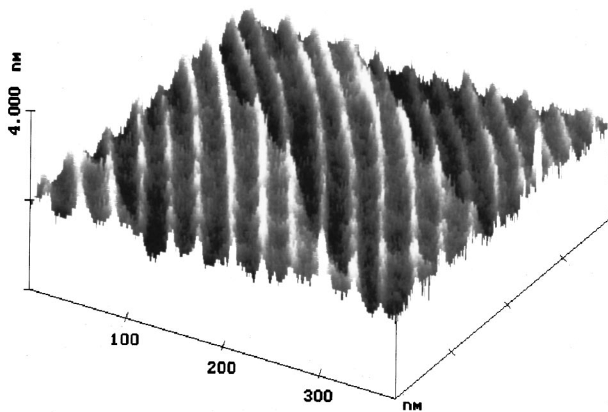

FIG. 7. Three-dimensional AFM image of 250 TiO_x lines fabricated by the SWNT AFM cantilever. Each line is 5 nm wide and 5 μm long. There is no degradation of the SWNT AFM cantilever, even after long oxidation.

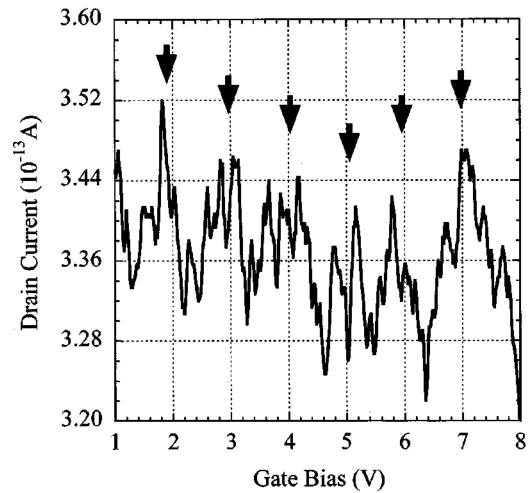

FIG. 8. Coulomb oscillation of SET fabricated by the SWNT AFM cantilever at room temperature. Drain bias was set at $V_D = 5.0$ V and gate bias was changed from $V_G = 1.0$ to 8.0 V.

The relative current oscillation dI/I in the Coulomb oscillation in Fig. 8 is as small as 5% because of the high-applied drain bias of $V_D = 5.0$ V. To get the higher relative current oscillation dI/I, the drain bias should be as small as possible. In the present device, however, owing to the large noise level, it was impossible to observe the Coulomb oscillation phenomena in the low drain bias.

The current oscillations are barely observable above the noise. In the several gate sweeps with the different drain bias conditions, the current still showed the oscillation peaks at almost the same gate bias position. Therefore, we could conclude that this drain current oscillation in Fig. 8 is not random fluctuations in noise, but is ''Coulomb oscillation.''

VI. CONCLUSIONS

The SWNT AFM cantilever grown directly onto the Si AFM cantilever was introduced into the AFM nano-oxidation process. Using the SWNT AFM cantilever, the ultranarrow TiO_x line of 5 nm width could be formed, and the SWNT AFM cantilever shows no degradation, even after long oxidation. From the result of the three-dimensional simulation, we found out that even if the width of the tunnel junction was changed, the tunnel-junction capacitance hardly changed. The SET fabricated by the SWNT AFM cantilever showed the Coulomb oscillation characteristic at room temperature. The periods of the oscillations were about 1 V. The gate capacitance was 1.6×10^{-19} F.

[1]K. Yano, T. Ishii, T. Hashimoto, T. Kobayashi, F. Murai, and K. Seki, Tech. Dig. Int. Electron Devices Meet. 541 (1993).
[2]K. Nakazato, T. J. Thornton, J. White, and H. Ahmed, Electron. Lett. **29**, 384 (1993).
[3]T. A. Fulton and G. J. Dolan, Phys. Rev. Lett. **59**, 109 (1987).
[4]K. Matsumoto, M. Ishii, K. Segawa, Y. Oka, B. J. Vartanian, and J. S. Harris, Appl. Phys. Lett. **68**, 34 (1996).

[5]K. Matsumoto, Proc. IEEE **85**, 612 (1997).
[6]K. Matsumoto, Y. Gotoh, T. Maeda, J. A. Dagata, and J. S. Harris, Tech. Dig. Int. Electron Devices Meet. 449 (1998).
[7]K. Matsumoto, S. Takahashi, M. Ishii, M. Hoshi, A. Kurokawa, S. Ichimura, and A. Ando, Jpn. J. Appl. Phys., Part 1 **34**, 1387 (1995).
[8]J. A. Dagata, T. Inoue, J. Itoh, K. Matsumoto, and H. Yokoyama, J. Appl. Phys. **84**, 6891 (1998).
[9]J. A. Dagata, T. Inoue, J. Itoh, and H. Yokoyama, Appl. Phys. Lett. **73**, 271 (1998).
[10]H. Dai, N. Franklin, and J. Han, Appl. Phys. Lett. **73**, 1508 (1998).
[11]E. B. Cooper, S. R. Manalis, H. Fang, H. Dai, K. Matsumoto, S. C. Minne, T. Hunt, and C. F. Quate, Appl. Phys. Lett. (to be published).
[12]R. J. Chen, H. Fang, N. R. Franklin, H. T. Soh, E. Chan, J. Kong, E. Cooper, S. Manalis, C. F. Quate, and H. Dai, Science (to be published).
[13]J. H. Hafner, C. L. Chueng, and C. M. Lieber, Nature (London) **398**, 761 (1999).
[14]J. H. Hafner, C. L. Chueng, and C. M. Lieber, J. Am. Chem. Soc. **121**, 9750 (1999).